

Direct measurement of the fine-structure interval of ^{27}Al in its ground 2P state

John M. Brown*

The Physical and Theoretical Chemistry Laboratory, South Parks Road, Oxford OX1 3QZ, England

Kenneth M. Evenson

Time and Frequency Division, National Institute of Standards and Technology, 325 Broadway, Boulder, Colorado 30303

(Received 23 November 1998; revised manuscript received 7 April 1999)

The $J = \frac{3}{2} \leftarrow \frac{1}{2}$ fine-structure transition in atomic ^{27}Al in its ground 2P state has been detected in the laboratory by far-infrared laser magnetic resonance. The fine-structure interval has been measured accurately as 3359.6228(17) GHz or 112.064 95(6) cm^{-1} . The spectra show the hyperfine structure associated with a nuclear spin of $\frac{5}{2}$ for ^{27}Al . The splittings are well reproduced by the hyperfine parameters determined earlier by atomic beam methods. The analysis of the laser magnetic-resonance spectra casts doubt on the published value for the Zeeman parameter $g_{3/2}$ also from the atomic beam measurements. Although the value determined in this paper is intrinsically much less accurate, it is in better agreement with the value obtained by a completely independent theoretical calculation. [S1050-2947(99)10307-X]

PACS number(s): 32.30.-r, 32.60.+i, 32.10.Fn

I. INTRODUCTION

The aluminum atom Al shows a regular fine-structure splitting in its ground 2P state, which arises from the $3s^23p^1$ electronic configuration. In this paper, we report a direct laboratory observation of the $J = \frac{3}{2} \leftarrow \frac{1}{2}$ fine-structure transition, which is magnetic dipole in character. The observation is made by laser magnetic resonance (LMR) in the far-infrared, and yields an accurate value for the splitting of $3\,359\,622.8 \pm 1.7$ MHz.

The fine-structure intervals of most first- and second-row atoms (including ions) in their ground states fall in the far-infrared region of the spectrum. A program to measure these intervals directly and accurately by LMR spectroscopy has been established at the Boulder laboratories of the National Institute of Standards and Technology. In these experiments, the atoms are generated in the gas phase by either chemical reactions or electric discharges. The design of the far-infrared laser in our spectrometer has been improved to increase its efficiency at short wavelengths; the short-wavelength limit of its operation is currently about 40 μm . Most of the fine-structure transitions which fall in this accessible range have now been measured (see, for example, Refs. [1–3]), including some metallic atoms. Aluminum is one of these.

Aluminum in its ground 2P state has been studied quite thoroughly by atomic beam magnetic resonance methods [4–8]. These measurements are very accurate and determine the nuclear hyperfine parameters (^{27}Al has a nuclear spin of $\frac{5}{2}$), and one of the two g factors ($g_{3/2}$). Hyperfine splittings have also been measured for aluminum in excited electronic states by optical spectroscopy, and are summarized in the review by Chang [8]; see also Ref. [9]. However, the fine-structure splitting in the ground 2P state has only been measured indirectly from comparatively inaccurate optical mea-

surements. The best available value is 112.061 ± 0.010 cm^{-1} , determined by Eriksson and Isberg [10]. Although aluminum does not appear to have been subjected to an *ab initio* theoretical study, Veseth reported some calculations of the ground-state g_J factors for several light atoms including Al [11]. Rather surprisingly, his value for $g_{3/2}$ does not agree very well with the experimental value [6].

In our program of determining the fine-structure intervals for light atoms directly, we have been motivated in many cases by the potential importance of these measurements for astronomers. The fine-structure transitions are commonly used to monitor local physical conditions in other parts of our galaxy [12,13]. This is not the case for aluminum which has a low cosmic abundance (3×10^{-6} relative to hydrogen [14]). Despite this, the atom has been identified in stellar atmospheres, including our own sun from optical transitions [10,15].

II. EXPERIMENTAL DETAILS

The principle of the LMR experiment is the detection of an atomic transition through the tuning of its frequency into resonance with a fixed-frequency laser by application of a variable magnetic field [16,17]. In the far-infrared region, the radiation source is a fixed-frequency, optically pumped laser. The lasing gas is excited to a chosen vibrational level by pumping with an appropriate line of an infrared laser, usually a CO_2 laser; in this way a population inversion is created. The molecules chosen to provide the gain medium therefore have absorption bands in the 10- μm region.

The far-infrared LMR spectrometer used in this work has been described elsewhere [18], and the details are not repeated here. We have improved the sensitivity of the apparatus by raising the Zeeman modulation frequency to 40 kHz. We have also modified the spectrometer to enhance its performance at wavelengths shorter than 100 μm by reducing the inside diameter of the polished copper pump tube from 50.8 to 19.1 mm (from 2 to $\frac{3}{4}$ in.). This provides a much better overlap between the pumped lasing gas and the far-

*Author to whom correspondence should be addressed. FAX: (44)-1865-275410. Electronic address: jmb@physchem.ox.ac.uk

TABLE I. Details of the far-infrared laser lines used to record magnetic resonance spectra of ^{27}Al in its ground 2P state.

Lasing gas	CO ₂ pump line	Wavelength (μm)	Frequency (MHz)
$^{13}\text{CH}_3\text{OH}$	9P(44)	88.95	3 370 404.8 ^a
CD_3OH	10P(20)	89.67	3 343 360.7 ^b
$^{13}\text{CD}_3\text{OD}$	10R(24)	90.15	3 325 304.6 ^c

^aMeasured for this work with an accuracy of 1.0 MHz.

^bReference [20], accuracy 1.0 MHz.

^cReference [21], accuracy 1.0 MHz.

infrared radiation field within the laser cavity, and many more short-wavelength laser lines can be made to oscillate as a result.

Some newly discovered far-infrared laser lines were used in this work. The frequencies of these laser lines were measured by mixing the far-infrared radiation with a pair of appropriately chosen, stabilized CO₂ laser lines on a fast metal-insulator-metal diode. The CO₂ lines are chosen so that their difference frequency is close to that of the far-infrared (FIR) laser; the resultant beat frequency in the microwave region is measured directly. The far-infrared frequency can be measured in this way to a relative accuracy of 1×10^{-8} . However, the main uncertainty comes from finding the center of the gain curve of the FIR lasing medium. That uncertainty is $\pm 2 \times 10^{-7}$ of the frequency; hence a second setting to the center of the gain curve has an uncertainty of $\pm 3 \times 10^{-7}$ of the laser frequency.

The aluminum atoms were generated in the sample region with a new microwave discharge source which has been developed specifically for the production of ions and other transient species. The details of its design and construction were given elsewhere [19]. The aluminum atoms were formed in the gas phase by dissociation of aluminum trimethyl, $\text{Al}(\text{CH}_3)_3$, entrained in helium gas, in the discharge. Under optimum conditions for production, the pressure of helium and $\text{Al}(\text{CH}_3)_3$ were 67 and 3.3 Pa (0.5 and 0.025 Torr) respectively; the discharge was a deep red-violet color.

The magnetic flux densities at which the resonances occurred were measured as accurately as possible, typically 0.01 mT for B less than 100 mT and 1×10^{-4} B over 100 mT. The magnetic field used in the experiment was stabilized with a rotating coil fluxmeter. This system was calibrated from time to time using a proton nuclear magnetic resonance probe.

III. RESULTS AND ANALYSIS

The fine-structure transition between the two spin components of the 2P ground state of Al has been observed with three separate far-infrared laser lines near the expected zero-field frequency (about 90 μm). The details of these lines are given in Table I. The spectra were readily identified as belonging to ^{27}Al because of the sextet hyperfine structure on each M_J transition, associated with the $I = \frac{5}{2}$ nuclear spin. An example of this hyperfine structure is shown in Fig. 1. The excellent signal-to-noise ratio is testimony to the very high sensitivity of the LMR experiment. An energy-level diagram which shows all the observed M_J transitions is given in Fig. 2. The spectra were readily assigned with the known values

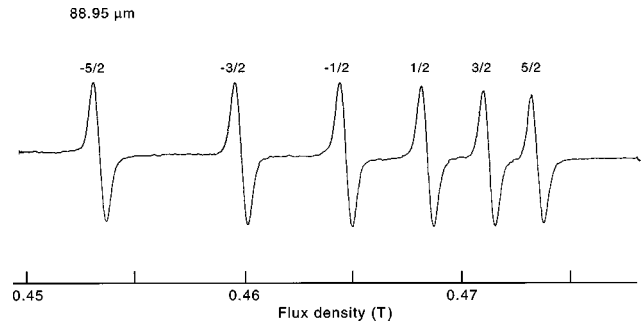


FIG. 1. Part of the far-infrared LMR spectrum of the Al atom recorded with the 88.95- μm laser line of $^{13}\text{CH}_3\text{OH}$ in perpendicular polarization. The output time constant of the lock-in amplifier was 0.1 s. The six-line pattern arises from the nuclear hyperfine structure for the ^{27}Al nucleus ($I = \frac{5}{2}$). The transitions obey the selection rule $\Delta M_J = 0$; each line is labeled by the value of M_J involved.

of the fine and hyperfine parameters. All of the observed signals obey the selection rule $\Delta M_F = \pm 1$ induced by perpendicular polarization ($B_\omega \perp B_0$ for magnetic dipole transitions). Transitions which obey $\Delta M_F = 0$ are also allowed with the correct orientation of the oscillating field B_ω , but are not observed in practice because the transitions $M_J = \pm \frac{1}{2} \leftarrow \pm \frac{1}{2}$ tune too slowly (4.67 MHz/mT) for them to be resonant with the laser lines used and with the maximum available laboratory field of 2.0 T.

In addition, on the 88.95- μm line, five weak, nuclear spin-forbidden lines were seen; they are shown in Fig. 3. These resonances obey the formal selection rules $\Delta M_J = +2$ and $\Delta M_J = -1$. They are observable because they occur at fairly low magnetic fields, and the nuclear hyperfine interactions are large for ^{27}Al .

The details of the observed resonances, including their measured values and assignments, are given in Table II.

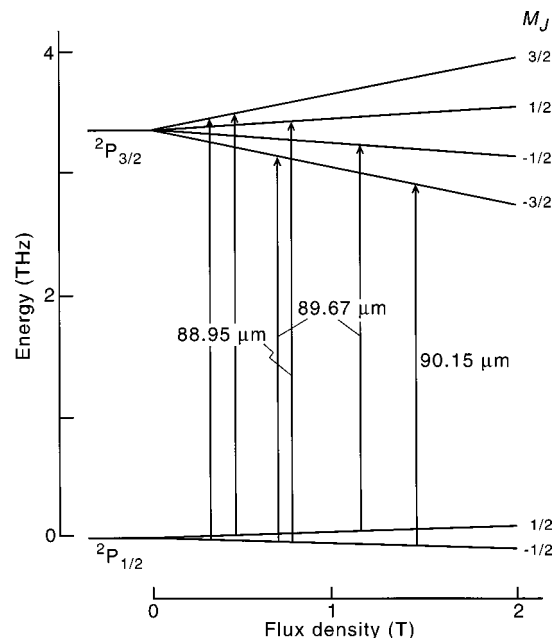


FIG. 2. Energy-level diagram for the Al atom in its ground 2P state, at zero field and in the presence of an applied magnetic field. The Zeeman splittings are exaggerated for the sake of clarity. The detected transitions are indicated at the observed magnetic fields.

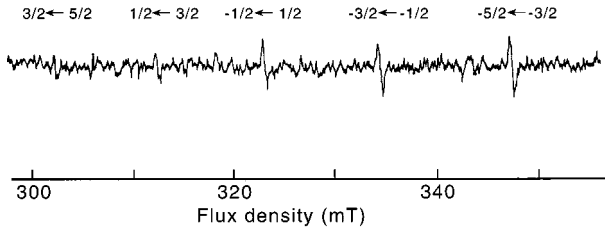


FIG. 3. The five nuclear spin-forbidden resonances observed in the far-infrared LMR spectrum of the Al atom. The spectrum was recorded in perpendicular polarization with the 88.95- μm laser line of $^{13}\text{CH}_3\text{OH}$; the output time constant was 0.1 s. All the resonances obey the formal selection rule $\Delta M_J = +2$; each resonance is labeled with its M_J quantum numbers. The increase in intensity across the pattern is consistent with theoretical expectation. These lines are predicted to be almost two orders of magnitude weaker than the allowed transitions shown in Fig. 1.

These measurements in the LMR spectrum have been analyzed with a standard effective Hamiltonian appropriate to a Russell-Saunders atom in an isolated electronic state, as first described by Radford, Hughes, and Beltrán-Lopez [22]. The effective Hamiltonian consists of four terms:

$$H_{\text{eff}} = H_{\text{fs}} + H_{\text{mhf}} + H_{\text{quad}} + H_{\text{Zeem}}, \quad (1)$$

where H_{fs} is the fine-structure term, H_{mhf} represents the magnetic hyperfine interaction, H_{quad} represents the nuclear electric quadrupole coupling, and H_{Zeem} represents the Zeeman interaction. There are, in general, electron spin-orbit and spin-spin contributions to H_{fs} , but, within the confines of a Russell-Saunders state, we can assign eigenvalues E_J^0 to H_{fs} corresponding to the energies of the unperturbed fine-

TABLE II. Observed resonances associated with the $^2P_{3/2} \rightarrow ^2P_{1/2}$ fine-structure transition of ^{27}Al .

Transition		M_I	ν (GHz)	B_0 (mT)	Obs.-calc. (MHz)	Tuning rate (MHz/mT)		
J	M_J							
3/2 ← 1/2	3/2 ← -1/2	3/2 ← 5/2	3370.4048	301.66	-0.8	32.7		
		1/2 ← 3/2		311.74	0.6	32.7		
		-1/2 ← 1/2		322.63	0.5	32.7		
		-3/2 ← -1/2		334.53	0.6	32.7		
		-5/2 ← -3/2		347.97	-0.9	32.7		
	3/2 ← 1/2	-5/2 ← -5/2	3370.4048	453.75	-0.4	-0.4	23.4	
		-3/2 ← -3/2		460.03	-0.2	-0.2	23.4	
		-1/2 ← -1/2		464.73	0.1	0.1	23.4	
		1/2 ← 1/2		468.44	-1.9	-1.9	23.4	
		3/2 ← 3/2		471.14	0.5	0.5	23.4	
		5/2 ← 5/2		473.25	1.6	1.6	23.4	
		1/2 ← -1/2	5/2 ← 5/2	3370.4048	713.94	0.1	0.1	14.0
			3/2 ← 3/2		732.75	-0.5	-0.5	14.0
			1/2 ← 1/2		752.74	0.7	0.7	14.0
			-1/2 ← -1/2		774.37	-0.5	-0.5	14.0
-3/2 ← -3/2			797.56	-0.4	-0.4	14.0		
-3/2 ← -1/2	-5/2 ← -5/2	3343.3607	822.43	2.4	2.4	14.0		
	-3/2 ← -3/2		685.37	-0.7	-0.7	-23.4		
	-1/2 ← -1/2		692.16	-0.5	-0.5	-23.4		
	1/2 ← 1/2		697.74	-1.1	-1.1	-23.4		
	3/2 ← 3/2		702.55	-0.7	-0.7	-23.4		
3/2 ← 1/2	-1/2 ← 1/2	5/2 ← 5/2	3343.3607	1110.58	-0.3	-0.3	-14.0	
		3/2 ← 3/2		1130.55	0.8	0.8	-14.0	
		1/2 ← 1/2		1150.93	0.3	0.3	-14.0	
		-1/2 ← -1/2		1171.93	0.5	0.5	-14.0	
		-3/2 ← -3/2		1193.52	0.1	0.1	-14.0	
	-3/2 ← -1/2	-5/2 ← -5/2	3325.3046	1215.83	0.0	0.0	-14.0	
		-3/2 ← -3/2		1459.94	1.9	1.9	-23.4	
		-1/2 ← -1/2		1465.36	1.1	1.1	-23.4	
		1/2 ← 1/2		1470.44	0.4	0.4	-23.4	
		3/2 ← 3/2		1475.22	-0.4	-0.4	-23.4	
		5/2 ← 5/2		1479.82	0.2	0.2	-23.4	
				14841.4	-1.0	-1.0	-23.4	

structure levels. The magnetic hyperfine structure term can be written compactly in spherical tensor notation as

$$H_{\text{mhf}} = 2g_I\mu_B\mu_N T^1(\mathbf{I}) \cdot \left\{ \langle r^{-3} \rangle_l T^1(\mathbf{L}) + g_S \frac{4\pi}{3} |\Psi(0)|^2 T^1(\mathbf{S}) - (10)^{1/2} g_S \langle r^{-3} \rangle_s \sum_i T^1(s_i, C_i^2) \right\}, \quad (2)$$

where the summation is over all open-shell electrons, and the other symbols have their usual meaning. The three contributions described in Eq. (2) are the nuclear-spin–electron-orbital interaction, the Fermi contact interaction, and the dipole-dipole coupling term, respectively. The electric quadrupole term has the form

$$H_{\text{quad}} = -eT^2(Q) \cdot T^2(\nabla\mathbf{E}), \quad (3)$$

where $eT^2(Q)$ is the nuclear electric quadrupole moment operator, and \mathbf{E} is the electric field at the nucleus arising from all the surrounding electronic charges. Finally, the Zeeman interaction is described by

$$H_{\text{Zeem}} = \{g_S\mu_B T^1(\mathbf{S}) + g_L\mu_B T^1(\mathbf{L}) - g_I\mu_N(1 - \sigma)T^1(\mathbf{I})\} \cdot T^1(\mathbf{B}) - \frac{1}{2}\chi_I B^2 - \chi_A \cdot T^2(\mathbf{L}, \mathbf{L})T^2(\mathbf{B}, \mathbf{B}), \quad (4)$$

where σ is the nuclear diamagnetic shielding constant, and χ_I and χ_A are the isotropic and anisotropic diamagnetic susceptibilities, respectively. The matrix elements of the three operators in Eqs. (2)–(4) are easy to evaluate for an atom in a state with well-defined values for the quantum numbers L , S , and J ; they have been given by several authors; see, for example, Cooksy and co-workers [23,24].

The experimental measurements for Al in a 2P state depend on the fine-structure interval $\Delta E_{3/2,1/2}$, the magnetic hyperfine and electric quadrupole parameters $A_{1/2}$, $A_{3/2}$, and B , and the g_J factors for the two levels concerned, $g_{1/2}$, and $g_{3/2}$. The observed resonances also depend very slightly on the off-diagonal hyperfine term $A_{3/2,1/2}$, linking the two spin components [7]. All of these parameters with the exception of the fine-structure interval and one g_J factor, $g_{1/2}$, have been determined much more accurately, by atomic beam measurements [6,7]. The three magnetic hyperfine parameters are linear combinations of the three radial expectation values in Eq. (2):

$$A_{1/2} = \frac{4}{3} g_I\mu_B\mu_N \left\{ 2\langle r^{-3} \rangle_l + g_S \langle r^{-3} \rangle_s - \frac{2\pi}{3} g_S |\Psi(0)|^2 \right\}, \quad (5)$$

$$A_{3/2} = \frac{2}{3} g_I\mu_B\mu_N \left\{ 2\langle r^{-3} \rangle_l - \frac{1}{5} g_S \langle r^{-3} \rangle_s + \frac{4\pi}{3} g_S |\Psi(0)|^2 \right\}, \quad (6)$$

$$A_{3/2,1/2} = \frac{1}{3} g_I\mu_B\mu_N \left\{ 2\langle r^{-3} \rangle_l - g_S \langle r^{-3} \rangle_s - \frac{8\pi}{3} g_S |\Psi(0)|^2 \right\}. \quad (7)$$

For an atom in a P electronic state with a nuclear spin greater than or equal to 1, there is a single electric quadrupole parameter

$$\begin{aligned} B &= -\frac{2}{(30)^{1/2}} \frac{eQ}{[2I(2I-1)]} \langle L \| T^2(\nabla\mathbf{E}) \| L \rangle \\ &= \frac{-eQ \langle L \| T^2(\nabla\mathbf{E}) \| L \rangle}{10(30)^{1/2}} \quad \text{for } {}^{27}\text{Al}. \end{aligned} \quad (8)$$

An initial fit of the data to determine values for $\Delta E_{3/2,1/2}$ and $g_{1/2}$, constraining the other parameters to their atomic

beam values, was disappointingly poor with some residuals greater than 10 MHz (an order of magnitude larger than the estimated experimental uncertainty). The fit was improved significantly by allowing the other g_J factor, $g_{3/2}$, to vary also. The optimal value for this parameter 1.333 81(2) was significantly smaller than the value of 1.334 74(5) determined from the atomic beam measurements of Ref. [6]. The quality of fit now corresponds to the expectations of experimental uncertainty.

The intrinsic accuracy of the atomic beam measurements is three orders of magnitude better than that of the far-infrared LMR measurement. Furthermore, we noted in earlier work [3,25] that systematic errors can arise in the determination of g_J factors in the LMR experiment if the atoms are formed (and detected) on the fringes of the far-infrared radiation field, in a region where the magnetic flux density is slightly smaller than the value in the center of the field gap. In normal circumstances, therefore, there would not be any justification for the reduction in the value of the $g_{3/2}$ mentioned above. However, a completely independent, *ab initio*, calculation of the two g_J factors for aluminum has reported by Veseth [11]. His value for $g_{3/2}$ of 1.334 065 is also considerably smaller than the value reported in Ref. [6]. With this encouragement, we decided to check carefully through the atomic beam measurements which are reported in the doctoral thesis of Martin [26].

Martin determined the value for $g_{3/2}$ for aluminum by measuring the frequency of a transition within the $F=4$ set of the $J=\frac{3}{2}$ component in a small but significant magnetic field. In the same set of measurements, he also determined the hyperfine splittings $F=4 \leftarrow 3$ and $F=3 \leftarrow 2$ in the $J=\frac{3}{2}$ level much more accurately than they had been measured earlier by Lew [4]. In addition, he reported a measurement of the other g factor, $g_{1/2}$, from a Zeeman measurement in the $J=\frac{1}{2}$ hyperfine levels. The value he determined, 0.666 24, had not been reported in the open literature before. It is also considerably larger than the value determined in the fit of our LMR data, 0.665 79(3), or the value calculated by Veseth of 0.665 845 [11].

A check of the numbers given in Martin's thesis [26] revealed no errors; the frequencies and parameters which he quoted are all consistent with each other. One slight difficulty in extracting values for the parameters for Al from his

TABLE III. Measurements of transitions within the fine-structure components of the 2P ground state of ^{27}Al made by atomic beam magnetic resonance.

J	Transition F	M_F	ν (MHz)	B_0 (mT)	Obs.-calc. (kHz)	Ref.
$\frac{1}{2} \leftarrow \frac{1}{2}$	$3 \leftarrow 2$	a	1506.1008(15) ^b	0.0	0.00	[7]
	$3 \leftarrow 3$	$-2 \leftarrow -3$	5.7314(3)	3.64176	0.0	[26]
$\frac{3}{2} \leftarrow \frac{3}{2}$	$4 \leftarrow 3$	a	392.2388(10)	0.0	0.02	[6,26]
	$3 \leftarrow 2$	a	274.3210(10)	0.0	-0.01	[6,26]
	$2 \leftarrow 2^c$	$-1 \leftarrow 0^c$	53.5239(10)	278.20	-0.06	[7]
	$4 \leftarrow 3^d$	$-1 \leftarrow -2^d$	48.6567(10)	220.40	-0.07	[7]
	$4 \leftarrow 4$	$-2 \leftarrow -3$	27.6709(7) ^e	3.66430	15.20	[6,26]

^aZero-field extrapolated value.

^bThe figures in parentheses represent the experimental uncertainty, as estimated by the referenced authors.

^cThis transition is more correctly described by its nuclear spin-decoupled quantum numbers, $M_J = -\frac{1}{2} \leftarrow -\frac{1}{2}$, and $M_I = -\frac{1}{2} \leftarrow -\frac{1}{2}$.

^dThis transition is more correctly described as $M_J = \frac{1}{2} \leftarrow \frac{1}{2}$ and $M_I = -\frac{3}{2} \leftarrow -\frac{5}{2}$.

^eThis data point is given zero weight in the fit.

data is that his measurements are all interrelated. We have therefore reanalyzed his data using our Russell-Saunders computer program, together with the three measurements by Harvey, Evans, and Lew [7]. The data used in the fit are collected in Table III. We have extrapolated Martin's measurements of the $F=4 \leftarrow 3$ and $3 \leftarrow 2$ hyperfine intervals in the $J=\frac{3}{2}$ level to zero field using Veseth's calculated values for the g factors [11]; this is a very short extrapolation and not very dependent on the g factors. We have also determined the flux densities at which Martin made his two g -factor measurements (see Table III); he simply gave the frequencies at these flux densities of known transitions in K and Al atoms. We have used these seven measurements to determine the magnetic and electric hyperfine parameters for aluminum in its ground 2P state. The g factors were constrained to Veseth's values, and the measurements of the transition for the $g_{3/2}$ factor were included at zero weight.

The resultant parameter values are given in Table IV. They are consistent with the previous determinations [6,7], but are slightly more reliable because we have used a full matrix representation of the eigenstates rather than first-order, algebraic formulas. Reference to the residuals in Table III shows that the transition frequency dependent on $g_{1/2}$ ($J=\frac{1}{2}$, $F=3 \leftarrow 3$, $M_F=-2 \leftarrow -3$) fits very well, whereas that which gives $g_{3/2}$ ($J=\frac{3}{2}$, $F=4 \leftarrow 4$, $M_F=-2 \leftarrow -3$) does not, with a residual of 15.2 kHz. This implies that the former is consistent with Veseth's value for $g_{1/2}$, whereas the latter is not consistent with his value for $g_{3/2}$. A shadow has therefore been cast over Martin's determination of the value for $g_{3/2}$ for aluminum (and over his value for $g_{1/2}$, since it depends directly on the other g factor in his analysis). Although his method is intrinsically very accurate, this discussion suggests that it should be checked independently.

The objective of the present work is to determine an accurate value for the fine-structure intervals for aluminum in its 2P ground state. In our final fit of the far-infrared LMR data, we constrained the nuclear hyperfine parameters to the values determined by the atomic beam data, given in Table IV, and allowed $\Delta E_{3/2,1/2}$ and the two g factors to vary. The parameter values determined in this way are also given in Table IV, with corresponding residuals in Table II.

IV. DISCUSSION

By the use of a far-infrared LMR measurement, we have made a direct measurement of the fine structure interval for ^{27}Al in its ground 2P state. The value obtained is 3359.6228(12) GHz or 112.064 95(4) cm^{-1} which is considerably more accurate than the previous value determined indirectly by Eriksson and Isberg [10] of 3359.50(30) GHz or 112.061(10) cm^{-1} . The numbers given here in parentheses are the estimated standard deviation of the fine-structure interval from the least-squares fit, that is, the *precision* of measurement. The *accuracy* of the present determination depends on (i) the resettability of the far-infrared laser to the top of its gain curve, and (ii) the accuracy of the field measurements. These two effects contribute independently to the total accuracy in a linear manner. The first contribution is

TABLE IV. Parameters determined for the fine and hyperfine levels of ^{27}Al in its ground 2P state.

Parameter	Present work	Previous values
$\Delta E_{3/2,1/2}$ (GHz)	3359.6228(12) ^{a,b}	3359.50(30) ^c
$A_{1/2}$ (MHz)	502.0346(5) ^d	502.0336(5) ^e
$A_{3/2}$ (MHz)	94.27723(10) ^d	94.27767(10) ^f
$A_{3/2,1/2}$ (MHz)	27.99(50) ^d	30.13(100) ^e
B (MHz)	9.45949(35) ^d	9.45763(35) ^f
$g_{1/2}$	0.66579(3) ^b	0.665845, ^g 0.66624(2) ^h
$g_{3/2}$	1.33381(2) ^b	1.334068, ^g 1.33474(5) ^f
g_I	1.456602	

^aThe figures in parentheses represent a 1σ estimate of the uncertainty in the parameter in units of the last quoted decimal place.

^bParameter value determined from a fit of the FIR laser magnetic-resonance data (Table II).

^cEriksson and Isberg [10].

^dParameter value determined in a refit of the atomic beam magnetic-resonance data (Table III).

^eHarvey, Evans, and Lew [7].

^fMartin, Sandars, and Woodgate [6].

^gVeseth [11].

^hMartin [26].

estimated to be 1.4 MHz ($\sqrt{2}$ times the measurement accuracy; see Table I). The second contribution from the magnetic-field measurement varies with the offset between the laser frequency and the fine-structure interval; it is the same for all resonances on a given laser line because the Zeeman effect is essentially linear. The field-dependent contribution to the accuracy is estimated to be 1.0, 1.6, and 3.5 MHz for the 88.95-, 89.67-, and 90.15- μm lines respectively. There are a large number of hyperfine components for each M_J transition recorded. However, the contribution to the overall accuracy from the hyperfine interactions is negligible because the parameters involved are well known from atomic beam work. When we take all these factors into account, the accuracy of the present determination of the fine-structure interval is estimated to be 1.7 MHz or $0.000\ 06\ \text{cm}^{-1}$.

In the course of our work, we have refitted the measurements on the hyperfine intervals in aluminum made by atomic beam resonance methods [6,7,26] to obtain improved values for the hyperfine parameters. The analysis of the LMR data has cast some doubt on the published value for the g factor $g_{3/2}$ [6]. The value determined from the LMR spectra is significantly smaller, and agrees much better with the theoretical value [11]. It is now well established that *ab initio* calculations of atomic g factors, particularly for light atoms, are very reliable [11,27,28].

The values of the parameters in Table IV can be used to

TABLE V. Zero-field frequencies and intensities for the fine-structure transitions in atomic aluminum in its ground 2P state.

Transition	Frequency/GHz	Relative intensity ^a	
$J = \frac{3}{2} \leftarrow \frac{1}{2}$	$F = 2 \leftarrow 3$	3358.6869(13) ^b	0.372
	$3 \leftarrow 3$	3358.9613(13)	1.302
	$4 \leftarrow 3$	3359.3535(13)	3.000
	$1 \leftarrow 2$	3360.0196(13)	1.005
	$2 \leftarrow 2$	3360.1930(13)	1.302
	$3 \leftarrow 2$	3360.4674(13)	1.042

^aThe relative intensity is given by the square of the magnetic dipole transition moment, $\langle LSJ'IF' || (\mathbf{m}/\mu_B) || LSJIF \rangle^2$.

^bEstimated *relative* uncertainty (1σ) in units of the last quoted decimal place. The accuracy of the predicted transitions is 1.7 MHz.

predict the hyperfine components of the fine structure transition of ^{27}Al ion its ground 2P state. The resultant spectrum is given in Table V.

ACKNOWLEDGMENTS

We are very grateful to Professor Pat Sandars for providing us with a copy of Dr. N. J. Martin's doctoral thesis, so that we could check through his calculations and, to some extent, reinterpret his data. This work was supported by NASA under Contract No. W-19, 167.

- [1] J. M. Brown, L. R. Zink, and K. M. Evenson, *Astrophys. J.* **423**, L151 (1994).
- [2] J. M. Brown, T. D. Varberg, K. M. Evenson, and A. L. Cooksy, *Astrophys. J.* **428**, L37 (1994).
- [3] J. M. Brown, L. R. Zink, and K. M. Evenson, *Phys. Rev. A* **57**, 2507 (1998).
- [4] H. Lew, *Phys. Rev.* **76**, 1086 (1949).
- [5] H. Lew and G. Wessel, *Phys. Rev.* **90**, 1 (1953).
- [6] N. J. Martin, P. G. H. Sandars, and G. Woodgate, *Proc. R. Soc. London, Ser. A* **305**, 139 (1968).
- [7] J. S. M. Harvey, L. Evans, and H. Lew, *Can. J. Phys.* **50**, 1719 (1972).
- [8] E. S. Chang, *J. Phys. Chem. Ref. Data* **19**, 119 (1990).
- [9] W. C. Martin and R. Zalubas, *J. Phys. Chem. Ref. Data* **8**, 817 (1979).
- [10] K. B. S. Eriksson and H. B. S. Isberg, *Ark. Fys.* **23**, 527 (1963).
- [11] L. Veseth, *Phys. Rev. A* **22**, 803 (1980).
- [12] E. L. Wright, J. C. Mather, C. L. Bennett, E. S. Cheng, R. A. Shafer, D. Fixsen, R. E. Eplee, Jr., R. B. Isaacman, S. M. Read, N. W. Boggess, S. Gulkis, M. G. Hauser, M. Janssen, T. Kelsall, P. M. Lubin, S. S. Meyer, S. H. Moseley, Jr., T. L. Murdock, R. F. Silverberg, G. F. Smoot, R. Weiss, and D. T. Wilkinson, *Astrophys. J.* **381**, 200 (1991).
- [13] M. R. Haas, D. Hollenbach, and E. F. Erickson, *Astrophys. J.* **374**, 555 (1991).
- [14] M. Rowan-Robinson, *Cosmology* (Clarendon, Oxford, 1981).
- [15] L. Delbouille, O. C. Mohler, and J. W. Swensson, *The Solar Spectrum from 3000 to 10000 Å* (Institut d'Astrophysique de l'Université de Liège, Observatoire Royal de Belgique, Liège, Belgium, 1973).
- [16] K. M. Evenson, *Faraday Discuss. Chem. Soc.* **71**, 7 (1981).
- [17] K. M. Evenson, R. J. Saykally, D. A. Jennings, R. F. Curl, Jr., and J. M. Brown, *Far Infrared Laser Magnetic Resonance*, edited by C. Bradley Moore, Chemical and Biochemical Applications of Lasers (Academic Press, New York, 1980), Vol. V, pp. 95–138.
- [18] T. J. Sears, P. R. Bunker, A. R. W. McKellar, K. M. Evenson, D. A. Jennings, and J. M. Brown, *J. Chem. Phys.* **77**, 5348 (1982).
- [19] T. D. Varberg, K. M. Evenson, and J. M. Brown, *J. Chem. Phys.* **100**, 2487 (1994).
- [20] E. C. C. Vasconcellos, S. C. Zerbetto, L. R. Zink, and K. M. Evenson (unpublished).
- [21] E. C. C. Vasconcellos, S. C. Zerbetto, L. R. Zink, and K. M. Evenson, *Int. J. Infrared Millim. Waves* **19**, 465 (1998).
- [22] H. E. Radford, V. W. Hughes, and V. Beltrán-Lopez, *Phys. Rev.* **123**, 153 (1961).
- [23] A. L. Cooksy, R. J. Saykally, J. M. Brown, and K. M. Evenson, *Astrophys. J.* **309**, 828 (1986).
- [24] A. L. Cooksy, D. C. Hovde, and R. J. Saykally, *J. Chem. Phys.* **84**, 6101 (1986).
- [25] J. M. Brown, H. Körsgen, and K. M. Evenson, *Astrophys. J.* **509**, 927 (1998).
- [26] N. J. Martin, Ph.D. thesis, Oxford University, 1965 (unpublished).
- [27] A. Abragham and J. H. Van Vleck, *Phys. Rev.* **92**, 1448 (1953).
- [28] M. Inguscio, K. M. Evenson, V. Beltrán-Lopez, and E. Ley-Koo, *Astrophys. J. Lett.* **278**, L127 (1984).